RSC Advances

ROYAL SOCIETY OF CHEMISTRY

www.rsc.org/advances

Cite this: DOI: 10.1039/c0xx00000x

www.rsc.org/xxxxxx

ARTICLE TYPE

Assembly of Zn-metal organic frameworks based on N-rich ligand: selective sorption for CO_2 and luminescence sensing of nitro explosives

Xiao-Li Hu, Chao Qin,* Liang Zhao, Fu-Hong Liu, Kui-Zhan Shao and Zhong-Min Su*

Received (in XXX, XXX) Xth XXXXXXXXX 20XX, Accepted Xth XXXXXXXXX 20XX

DOI: 10.1039/b000000x

Two novle Zn(II) coordination polymer compounds, namely, $[Zn_3(HL)_2(fma)_2]\cdot DMA\cdot H_2O$ (**1**) and $[Zn_2(\mu_3\text{-}OH)(HL)(Br\text{-}bdc)]\cdot 0.5DMA\cdot CH_3OH\cdot H_2O$ (**2**) have been successfully obtained with1-(5-tetrazolyl)-4-(1-imidazolyl) benzene ligand and dicarboxylic acids (fma = fumaric acid; Br-bdc = 2-bromoterephthalic acid). Compound **1** exhibits a 3D framework with square aperture diameter for the channel is 8.8 × 8.8 $Å^2$, and the framework can be simplified as a (3,4)-connected **tfj** network with the point symbol of $\{4.8^2\}_4\{4^2.8^4\}_2\{8^4.12^2\}$ topology. In compound **2**, the HL ligand form a 2D sheet of Zn(HL) by linking Zn ions along the *c* axis, which are further connected by double Br-bdc pillars resulting in unique bi-pillared-layer type 3D frameworks. The result **1a** exhibits a certain degree of CO_2 uptakes and selective CO_2/N_2 adsorption capacity. Furthermore, luminescent properties of **1a** well dispersed in different solvents have also been investigated systematically, which demonstrate distinct solvent-dependent luminescent spectra with emission intensities significantly quenched toward acetone and nitrobenzene.

Introduction

Recently, metal–organic frameworks (MOFs) have developed into a blue-chip research field not only because of their structural and topological diversities but also for their diverse potential applications in gas adsorption, catalysis and selective separation.[1-4] Tetrazole and its derivatives have been widely employed in the construction of cocrystals and metal–organic frameworks due to their versatile bridging modes.[5] In particular, a number of coordination polymers with interesting structural and/or physical properties, such as luminescence, non-linear optics, ferroelectricity, magnetism and porosity, have been synthesized from ligands bearing one or more tetrazoles.[6,7] On the other hand, aiming at practical applications, the selected MOF adsorbents must sustain their stability and crystallinity under ambient conditions, even for water and humid air. Compared with the majority of carboxylate-based MOFs, azolate-based MOFs (also known as metal azolate frameworks) often exhibit superior stability.[8] In this work, the ligand HL = 1-(5-tetrazolyl)-4-(1-imidazolyl)benzene) was employed as building blocks, which has several remarkable features as follows: (a) the rigid skeleton and azolate-based configuration may tend to construct MOFs with high stability; (b) five potential coordination sites in the HL ligand are able to exhibit versatile bridging modes to satisfy geometric requirement of metal centers; (c) the HL is a bifunctional N-donors ligand, thus, polycarboxylate ligands as bridging rods can be introduced into reaction system to enrich the coordination patterns.

So far, the MOF chemosensors have obtained considerable attention owing to their intriguing photo-physical properties, such as evident Stokes shifts, excitation in the visible range and relatively long lifetimes.[9] Luminescent MOFs can be applied in the detection of hazardous substances, which is a very important aspect in terms of environmental and safety considerations. Several transition metal–organic frameworks used for molecular sensing have also been reported, for example, the sensing of nitric oxide in Cu−TCA,[10] detection of high explosives and other aromatics in $[Zn_2(oba)_2(bpy)]$ [H_2oba = 4,4′-oxybis(benzoic acid); bpy = 4,4′-bipyridine].[11] The design and synthesis of MOF sensors aimed at the convenient detection of volatile organic solvent molecules, especially nitro explosives, have attracted tremendous interest in coordination chemistry.

In this work, two novel coordination polymers with diverse structures have been solvothermally synthesized using HL ligand and dicarboxylate acids, namely, $[Zn_3(HL)_2(fma)_2]\cdot DMA\cdot H_2O$ (**1**) and $[Zn_2(\mu_3\text{-}OH)(HL)(Br\text{-}bdc)]\cdot 0.5DMA\cdot CH_3OH\cdot H_2O$ (**2**). Compound **1** exhibits square channels, which can be described as 3D (3,4)-connected **tfj** network with the point symbol of $\{4.8^2\}_4\{4^2.8^4\}_2\{8^4.12^2\}$ topology. Compound **2** shows a bi-pillared-layer type 3D framework based on 2D sheet of Zn(HL) and double Br-bdc pillars. **1a** exhibits a certain degree of CO_2 uptakes and selective CO_2/N_2 adsorption capacities. Luminescent properties of activated **1a** dispersed in different solvents have been investigated systematically, which demonstrate distinct solvent-dependent luminescent spectra with emission intensities significantly quenched toward acetone and nitrobenzene.

Experimental

Materials and physical measurements: All chemical materials were purchased from commercial sources and used without

Table 1 Crystal data and structure refinements for **1**.

	1	**2**
Formula	$C_{32}H_{29}N_{13}O_{10}Zn_3$	$C_{21}H_{19.5}N_{6.5}O_{7.5}BrZn_2$
Formula weight	951.9	693.64
Crystal system	monoclinic	monoclinic
Space group	*C*2/*c*	$P2_1/c$
a (Å)	20.861(5)	16.279(5)
b (Å)	15.959(5)	6.820(5)
c (Å)	13.286(5)	23.711(5)
α (°)	90.000(5)	90.000(5)
β (°)	96.789(5)	103.970(5)
γ (°)	90.000(5)	90.000(5)
V (Å^3)	4392(2)	2555(2)
Z	4	4
$D_{calcd.}$[gcm^{-3}]	1.280	1.565
F(000)	1696	1176
Reflections collected	12423/3858	13945/4489
R(int)	0.0564	0.0383
Goodness-of-fit on F^2	1.063	1.058
R_1[a] [$I>2\sigma(I)$]	0.0471	0.0550
wR_2[b]	0.1168	0.1647

[a] $R_1 = \sum||F_o| - |F_c||/\sum|F_o|$, [b] $wR_2 = |\sum w(|F_o|^2 - |F_c|^2)^2/\sum|w(F_o^2)^2|^{1/2}$

further purification. The FT-IR spectra were recorded from KBr pellets in the range 4000–400 cm^{-1} on a Mattson Alpha-Centauri spectrometer. XRPD patterns were recorded on a Siemens D5005 diffractometer with Cu Kα (λ = 1.5418 Å) radiation in the range of 3−60° at a rate of 5°/min. The UV-Vis absorption spectra were examined on a Shimadzu UV-2550 spectrophotometer in the wavelength range of 200-800 nm. The C, H, and N elemental analyses were conducted on a Perkin-Elmer 2400 CHN elemental analyzer. TG curves were performed on a Perkin–Elmer TG-7 analyzer heated from room temperature to 1000 ºC at a ramp rate of 5 °C/min under nitrogen. The photoluminescence spectra were measured on a Perkin-Elmer FLS-920 Edinburgh Fluorescence Spectrometer.

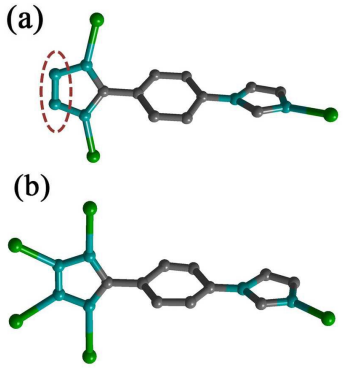

Scheme 1. The Coordination modes of L^- appearing in **1** (a) and **2** (b).

Synthesis

Preparation of $[Zn_3(HL)_2(fma)_2]\cdot DMA\cdot H_2O$ (1)

A mixture of $Zn(NO_3)_2\cdot 6H_2O$ (60 mg, 0.2 mmol), HL (21 mg, 0.1 mmol), and fma (14 mg, 0.1 mmol) was dissolved in 6 mL of DMA (N,N-Dimethylacetamide)/MeOH (methanol)/H_2O (1:1:3, v/v/v). The final mixture was placed in a Parr Teflon-lined stainless steel vessel (15 mL) under autogenous pressure and heated at 100 °C for 3 days. Colorless crystals were obtained, which were washed with mother liquid, and dried under ambient conditions. Elemental analysis: Anal. Calcd for $C_{32}H_{29}N_{13}O_{10}Zn_3$: C, 40.38; H, 3.07; N, 19.13. Found: C, 40.05; H, 2.75; N, 18.88. IR (KBr, cm^{-1}):1150.83 (w), 534.92 (w), 623.34 (w), 1040.02 (w), 1007.56 (w), 552.09 (w), 784.08 (w), 1225.64 (w), 449.41 (w), 476.67 (w), 946.92 (w), 711.09 (w), 1471.88 (w), 1124.20 (w), 3431.54 (w), 655.95 (w), 760.83 (w), 1395.39 (m), 3110.81 (m), 1068.30 (m), 1037.37 (m), 966.61 (m), 1261.87 (m), 1614.22 (s), 1312.03 (s), 845.57 (s), 1453.28 (s), 1544.73 (s), 1512.73 (s).

Preparation of $[Zn_2(\mu_3\text{-}OH)(HL)(Br\text{-}bdc)]\cdot 0.5DMA\cdot CH_3OH\cdot H_2O$ (2)

The synthetic procedure is similar to that of **1** except that the fma (14 mg, 0.1 mmol) was replaced by Br-bdc (24 mg, 0.1 mmol). The final mixture was placed in a Parr Teflon-lined stainless steel vessel (15 mL) under autogenous pressure and heated at 120 °C for 3 days. Colorless crystals were obtained, which were washed with mother liquid, and dried under ambient conditions. Elemental analysis: Anal. Calcd for $C_{21}H_{19.5}N_{6.5}O_{7.5}BrZn_2$: C,

36.37; H, 2.83; N, 13.13. Found: C, 36.02; H, 2.62; N, 12.80. IR (KBr, cm^{-1}):1159.42 (w), 444.93 (w), 533.29 (w), 1010.72 (w), 499.41 (w), 945.45 (w), 1138.52 (w), 559.96 (w), 731.71 (w), 1195.54 (w), 1124.17 (w), 965.66 (w), 1035.92 (w), 779.06 (w), 651.33 (w), 1063.37 (m), 1251.98 (m), 1458.19 (m), 1313.13 (m), 1488.64 (s), 1510.40 (s), 3148.98 (s), 3388.51 (s), 1542.90 (s), 1587.24 (s).

Single crystal X-ray diffraction

Single-crystal X-ray diffraction data for **1-2** were recorded on a Bruker Apex CCD II area-detector diffractometer with graphitemonochromated Mo-Kα radiation (λ = 0.71073 Å) at 296(2) K. Absorption corrections were applied using multi-scan technique. Their structures were solved by the direct method of SHELXS-97 and refined by full-matrix least-square techniques with the SHELXL-97 program.[12] Because guest molecules in the channels of **1-2** were highly disordered and could not be modeled properly, the SQUEEZE routine of PLATON was applied to remove their contributions to the scattering.[13] The reported refinements are of the guest-free structures obtained by the SQUEEZE routine, and the results were attached to the CIF file. The crystal data and structure refinement results of **1-2** are summarized in Table 1.

Gas sorption experiments

The N_2 and CO_2 sorption measurements were performed on automatic volumetric adsorption equipment (Belsorp mini II). Before gas adsorption measurements, the samples were immersed in CH_2Cl_2 for 24 h, and the extracts were decanted. Fresh CH_2Cl_2 was subsequently added, and the crystals were allowed to stay for an additional 24 h to remove the nonvolatile solvates (DMA). After the removal of dichloromethane by decanting, the samples were activated by drying under a dynamic vacuum at room temperature overnight. Before the measurement, the samples were dried again by using the 'outgas' function of the surface area analyzer for 12 h at 90 ºC.

Results and discussion

Crystal structure descriptions

Crystal structure of $[Zn_3(HL)_2(fma)_2]\cdot DMA\cdot H_2O$ (1)

Compound **1** crystallizes in the monoclinic space group *C*2/*c*, and the asymmetric unit contains one HL, one fma ligand and two Zn(II) ions. As depicted in Fig 1, Zn1 atom is four-coordinated by one imidazolyl N atom, one tetrazolyl N atom from two different HL ligands and two O atoms from two distinct fma ligands, to give a distorted tetrahedral geometry. The two Zn1−O bond lengths are both 1.955 (3) Å and the Zn1−N bond lengths are both 2.001 (4) Å. The coordinating bond angles around the Zn1 are in the range of 91.47(18) to 120.10 (14)º. Zn2 atom also shows four-coordinated, with the tetrahedral coordination geometry, by two tetrazolyl N atom from two different L^- ligands and two carboxylate O atoms from two individual fma ligands. The Zn2−O bond lengths are in the range of 1.915 (4) -1.972 (3) Å, and the Zn2−N bond lengths are in the range of 1.984 (4) - 2.015 (4) Å, the bond angles around the Zn2 ranged 101.20 (14)

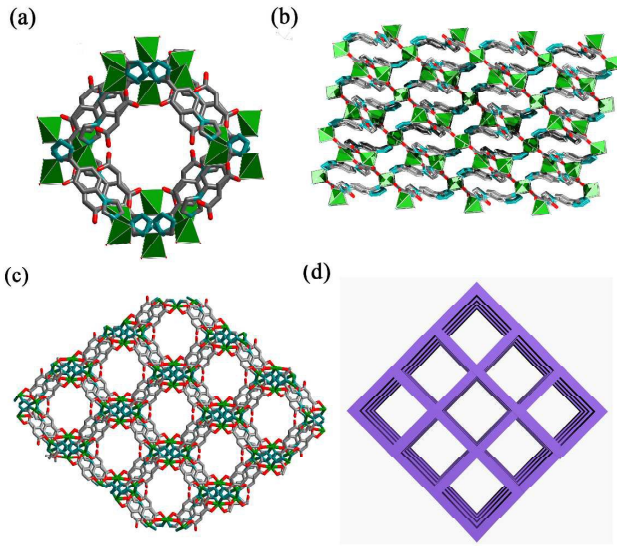

Fig. 1 (a) The single channel for **1**. (b) The wavelike 3D framework of **1** looking long the *b* axis. (c) The view and (d) Schematic representation of square channel of **1** along the *c* axis.

to 118.16 (18)º. In compound **1**, each tetrazolyl group in L^- ligand links two metal ions and each imidazolyl coordinates to a metal ion, and thus the L^- can be described as μ3-bridge. Evidently, two tetrazolyl N atoms of each ligand molecules do not take part in coordination to Zn(II) centers, that is, there are uncoordinated nitrogen atoms from the N-rich aromatic ligand. The fma^{2-} ligand adopts μ^1-η^1:η^0-monodentate carboxylate coordination mode and connects two different metal ions as μ_2-bridge. In a word, each L^- ligand bridges three metal ions and each metal ion is surrounded by two L^- ligands and two fma^{2-} liangds. This kind of interconnection extends in finitely to form a 3D network. From *c* axis, the square aperture diameter for the channel is 8.8 × 8.8 $Å^2$ (*a* × *b*). The solvent accessible volumes of 38.5 % (1691.9 $Å^3$) per unit cell (4392.2 $Å^3$), is calculated by PLATON.[14] Topological analysis shows that Zn atoms can be defined as 4-connected nodes, and L^- ligand defined as 3-connected nodes, the architecture of **1** that can be simplified as

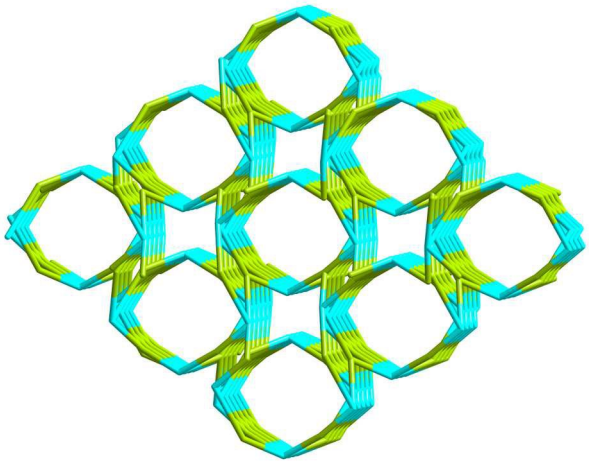

Fig. 2 Schematic representation of the (3,4)-connected nets with the point symbol of $\{4.8^2\}_4\{4^2.8^4\}_2\{8^4.12^2\}$.

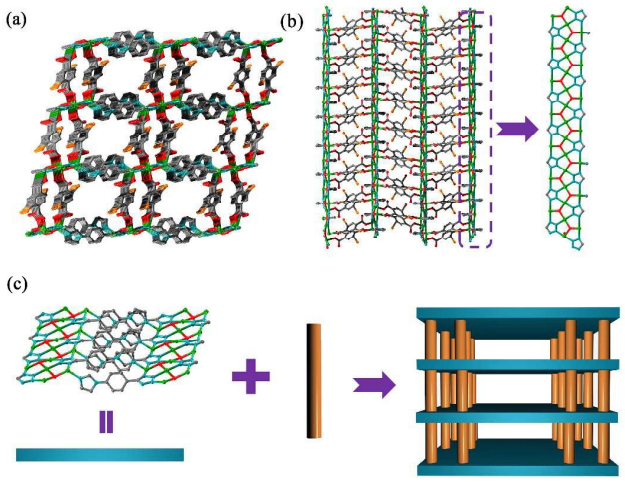

Fig. 3 (a) View of 3D coordination framework along the *c* axis. (b) The representation of 1D chain and View of 3D coordination framework along the *b* axis. (c) Schematic representations of bi-pillared-layer framework.

(3,4)-connected **tfj** network with the point symbol of $\{4.8^2\}_4\{4^2.8^4\}_2\{8^4.12^2\}$.[15]

Crystal structure of $[Zn_2(\mu_3\text{-OH})(HL)(Br\text{-bdc})]\cdot 0.5DMA\cdot CH_3OH\cdot H_2O$ (2)

The structure of **2** features a 3D bipillared-layer framework. Single-crystal X-ray analysis indicates that the architectures of **2** crystallizes in monoclinic, space group $P2_1/c$. There exist two types of crystallographically independent Zn(II) ions, one HL ligand and one Br-bdc ligand. As displayed in Fig. 3, Zn1 penta-connected to one tetrazolyl N atom, one imidazolyl N atom of two different HL ligands, one oxygen atom from Br-bdc ligand and two μ_3-OH groups. Zn2 shows a trigonal bipyramidal geometry by linking two tetrazolyl N atoms from two distinct HL ligands, one μ_3-OH group, leaving the remaining coordination sites occupied by one Br-bdc ligand. The Zn1-Zn2 units are connected repeatedly by N atom from tetrazolyl to form a 1D chain that extends along the *c* axis (Fig. 3b). Each tetrazolyl group in L^- ligand links two Zn1 and two Zn2 atoms, each imidazolyl group coordinates to one Zn1 ion, forming a perfectly 2D planar Zn(HL) sheet paralleling with the crystallographic *ab* plane (Fig. 3c). Each 2D sheet further pillared by the Br-bdc resulting in a 3D pillared layer network. It is worth to mention that the two independent Zn(II) centers of the 2D sheet are pillared by the double column of Br-bdc forming a bi-pillared-layer framework. In the whole structure of **2**, the HL ligand displays five coordination sites. In the layer, the nearest Zn1-Zn2 distance is 3.52 Å and the nearest Zn2-Zn2 distance is 3.42 Å. Calculations using PLATON show that the effective pore volume for **2** is about 21.3% (545.5 $Å^3$) per unit cell (2566.0 $Å^3$), which is occupied by solvent guests.

Powder XRD patterns and Thermal properties

In order to confirm the phase purity of **1-2**, we measured the powder X-ay diffraction at room temperature (Fig. S6-S7). The experimental X-ray diffraction patterns compared to the

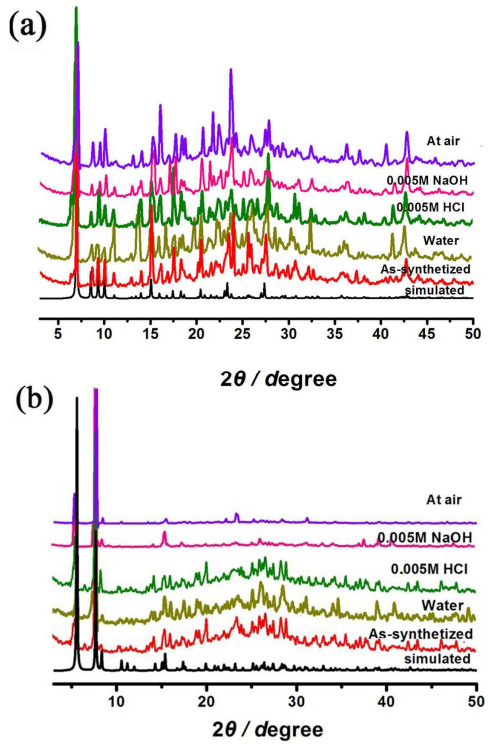

Fig. 4 X-ray powder diffraction patterns of **1** (a) and **2** (b): simulated (black), as-synthesized (red), treated in water (yellow), HCl (0.005 M, green), NaOH (0.005 M, pink) and exposed in air (purple).

corresponding simulated patterns calculated based on single crystal diffraction data, which indicates that all the samples were in a pure phase. To study the thermal stability of the compounds, thermogravimetric analyses (TGA) were performed on polycrystalline samples under nitrogen atmosphere with a heating rate of 10 °C min^{-1} (Fig. S8-S9). The TG diagram of **1** displays two distinct weight losses, the first loss of 11.0 % from 50 to 271 °C, in agreement with the weight of DMA and H_2O molecules (calcd 10.2 %). The frameworks collapsed in the temperature around 330 °C. TGA curve of **2** reveals the first weight loss 13.2 % is from 35 to 284 °C and corresponds to the loss of the solvents, then starts to decompose after 337 °C.

As we know, a good gas storage (or separation) material must be stable toward moisture in practical applications, and azolate-based MOFs often exhibit excellent framework stability. Thus, the chemical stability is examined by suspending crystals of **1** and **2** in water and acidic (0.005 M HCl) or basic (0.005 M NaOH) aqueous solutions for 12 h, their XRPD patterns keep the same peak positions. However, **1a** was performed N_2 sorption studies after water, HCl (0.005 M) and NaOH (0.005 M) treatment, in order to further testify the stability of MOFs. The N_2 adsorptions showed adsorption amount have a decrease (Fig. S11). It can be explained that water and acid/alkaline solutions destroyed the framework in a certain degree, although XRPD patterns keep the same. In addition, the overall frameworks of **1-2** are maintained after placing the samples in air for even 2 months (Fig. 4). The chemical stability is also examined by suspending crystals of **2** in boiling solvent, such as acetone, acetonitrile, N-methyl-2-pyrrolidone (NMP), N, N-dimethyl ethanolamine, THF, ethyl acetate and *n*-hexane, the powder X-ray diffraction (PXRD)

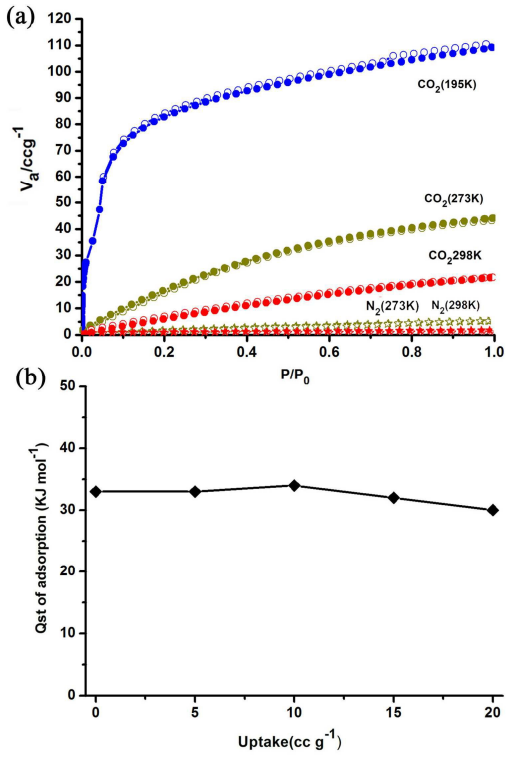

Fig. 5 (a) CO_2 and N_2 sorption isotherms for **1a** at 273, 298 K and 195K. (b) Isosteric heats of CO_2 adsorption (Q_{st}) for **1a**.

patterns have similar shape and intensity (Fig. S10).

Gas adsorption properties

Because of the porosity (38.5 %) and the uncoordinated nitrogen atoms of **1**, we select **1** as an example to explore the N_2 and CO_2 adsorption. The activated samples were prepared by exchanging the solvent in the as-synthesized **1** with CH_2Cl_2, followed by evacuation under vacuum. Samples of **1** were evacuated under vacuum at room temperature over night to completely remove the solvent CH_2Cl_2 molecules and thus to form guest-free phases **1a**. The architectural stability and permanent porosity of **1a** were confirmed by measuring the N_2 adsorption experiments at 77 K, displaying type I adsorption isotherms characteristic of microporous solids. The nitrogen adsorptions showed good reversibility. The N_2 adsorption amounts of **1a** at 1 bar were about 54.8 cm^3 g^{-1} (Fig. S11). For **1a**, the apparent BET area was 138 m^2 g^{-1}, based on the nitrogen adsorption isotherm.

Subsequently we carried out CO_2 adsorption experiments on **1a**. As shown in Fig. 5, the CO_2 sorption isotherms for **1a** were measured at 273, 298 K and 195K, respectively. **1a** have CO_2 uptakes at 1 bar with saturation of 108.7 cm^3/g at 195 K, 43.2 cm^3/g at 273 K and 21.0 cm^3/g at 298 K (Fig. 5a). For **1**, the isosteric heats of adsorption (Q_{st}) of CO_2 were calculated by using the Clausius–Clapeyron equation to quantitatively evaluate the binding strengths.[16] The Q_{st} at zero coverage of CO_2 of **1** was about 33 KJ mol^{-1}, thus indicating strong interactions between CO_2 and the framework. Meanwhile, the enthalpy of CO_2 adsorption (Q_{st}) was calculated using the virial equation[17] from the adsorption isotherms recorded at 273 and 298 K (Fig. S12). **1** exhibits a strong binding affinity for CO_2 (around 35.4 kJ mol^{-1}) at zero coverage, which is quite close to the value calculated by Clausius–Clapeyron equation (around 33 kJ mol^{-1}). Unexpectedly, the CO_2 uptakes for **1a** are quite high while N_2 sorption was hardly adsorbed at 273 and 298 K (Fig. 5a).

Photoluminescent investigation

Recently, metal-organic frameworks constructed from d^{10} metal ions and conjugated organic linkers are promising candidates for potential photoactive materials. Therefore, to see their luminescent behavior, the emission properties of dicarboxylate ligands and HL ligand along with compounds **1-2** were

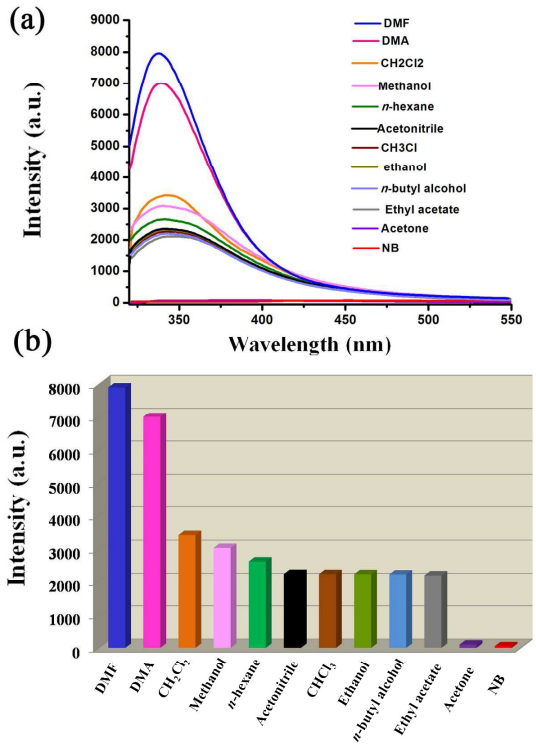

Fig. 6 Comparisons of the luminescence intensity of **1a**-solvent emulsions at room temperature (excited at 301 nm) (solvent = DMA, DMF, MeOH, *n*-hexane, Ethyl acetate, CH_3Cl, EtOH, *n*-butyl alcohol, Acetonitrile, Acetone, CH_2Cl_2, and Nitrobenzene).

investigated in the solid state at room temperature (Fig. S13-S16). The HL ligand shows emission peak at 340 nm (λ_{ex} = 275 nm). The excitation of **1-2** at 319 nm and 316 nm resulted in a strong emission band at 371 nm and 419 nm. The emissions for **1-2** are probably assigned to be the ligand centered π–π* or n–π* fluorescence due to their close resemblance of the emission bands of HL ligand.[18]

Compared to **2**, **1** has the stronger emission band, so we selected **1** to examine the luminescent property in different solvent emulsions. The solvents used are dichloromethane (CH_2Cl_2), trichloromethane ($CHCl_3$), acetonitrile, ethanol, methanol, *n*-hexane, ethyl acetate, N, N-dimethylformamide (DMF), N, N-dimethylacetamide (DMA), acetone, *n*-butyl alcohol and and nitrobenzene. The most interesting feature is that its PL spectrum is largely dependent on the solvent molecules, particularly in the case of acetone and nitrobenzene, which

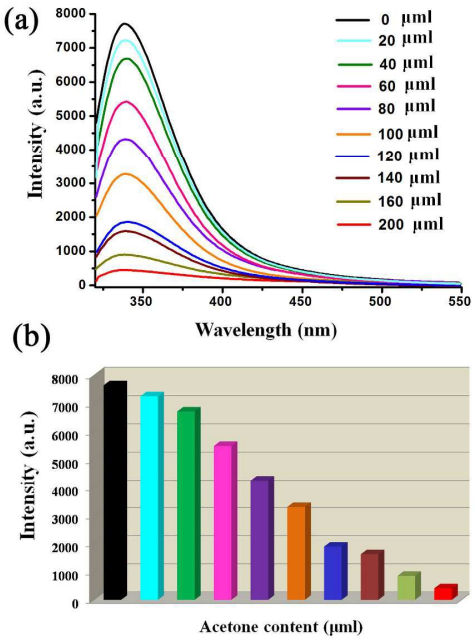

Fig. 7 Emission spectra of the dispersed **1a** in DMF in the presence of various contents of acetone solvent (excited at 301 nm).

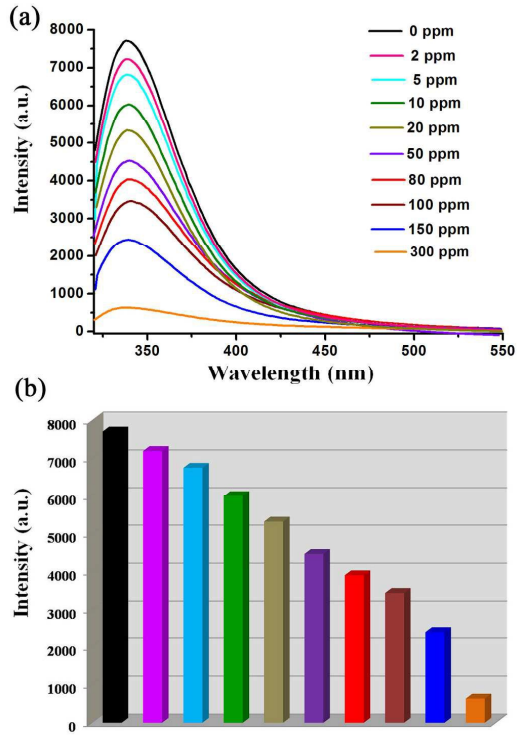

Fig. 8 Emission spectra of **1a** at different nitrobenzene (NB) concentrations in DMF (excited at 301 nm).

exhibit the most significant quenching effects (Fig. 6). Such solvent-dependent luminescence properties are of interest for the sensing of acetone and nitrobenzene solvent molecules.

The emission spectra are recorded by the gradual addition of acetone solution into a suspension of 0.3 mg of **1a** dispersed in 3 mL of DMF solution. When the acetone solvent content was

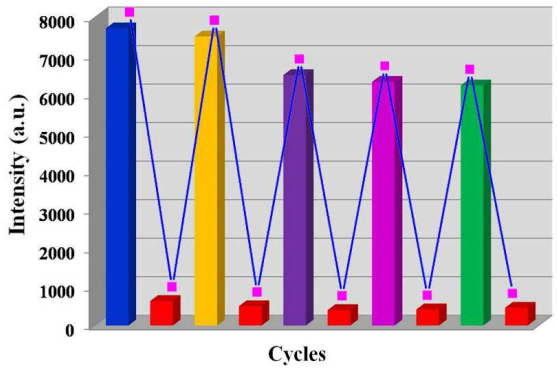

Fig. 9 The quenching and recyclability test of **1a** upon addition of 300 ppm of DMF solution of NB.

gradually added and increased to **1a**-DMF standard emulsion, the fluorescence intensity of the standard emulsion gradually decreased with the addition of acetone solvent (Fig. 7). The quenching efficiency was estimated to be 93.8 % for adding 200 µml acetone. The fluorescence decrease was nearly proportional to the acetone concentration and the system ultimately reaches the equilibrium state. The efficient quenching of acetone in this system can be ascribed to the physical interaction of the solute and solvent, which induces the electron transfer from the excited **1a** to electron-deficient acetone.[19]

A batch of emulsions of **1a** in DMF with gradually increased nitrobenzene concentration was prepared to monitor the emissive response. As seen in Fig. 8, the luminescent intensity of theemulsions significantly decreased with increasing addition of nitrobenzene. The intensity of **1a**-DMF standard emulsion decreased to 51 % at only 80 ppm, 8 % at 300 ppm, which allowed us to detect small amounts of nitrobenzene in solution. Additionally, we also found that **1a** can be regenerated and reused for five numbers of cycles by centrifugation of the solution after use and washing several times with DMF (Fig. 9). The quenching efficiencies of every cycle are basically unchanged through monitoring the emission spectra of **1a** dispersed in the presence of 300 ppm nitrobenzene in DMF. The PXRD patterns of the initial sample and recovered sample after five cycles of quenching and recovery also indicate the high stability of this compound (Fig. S17). The result reveals that **1** could be applied as a fluorescence sensor for NB with high sensitivity, selectivity, and recyclability.

The luminescence quenching may be due to the photoinduced electron-transfer (PET) mechanism. The electron-transfer progress can be interpreted by inductive effect. The nitrobenzene with electron-deficient property can obtain an electron from excited ligand, which has been confirmed by molecular orbital theory.[20] The frontier molecular orbitals of nitrobenzene and the ligand are calculated by density functional theory at the level of B3LYP/6-31G*.[20] The LUMO of nitrobenzene is low-lying π*-type orbital stabilized by the -NO_2 through conjugation, so it is lower than LUMO of HL ligand (Fig. 10). Therefore, the excited state electrons can transfer from MOF to nitrobenzene, which leads to luminescence quenching.

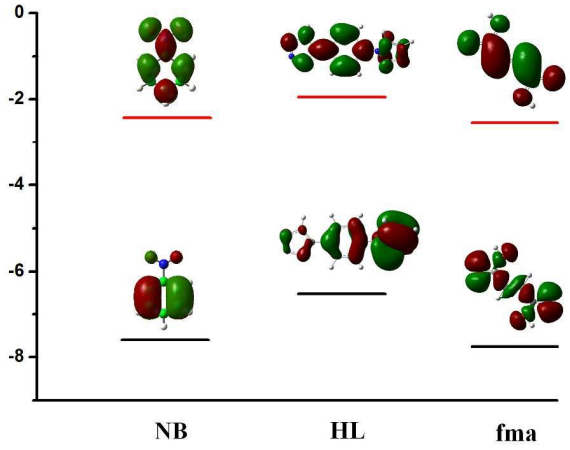

Fig. 10 Shapes of HOMO and LUMO of the molecular orbitals considered and the relative energy level investigated by the B3LYP/6-31G* method.

Conclusion

In summary, two novel MOFs assembled by 1-(5-tetrazolyl)-4-(1-imidazolyl) benzene and dicarboxylate ligangs have been synthesized and characterized. **1** exhibits a 3D framework with square aperture diameter for the channel is 8.8 × 8.8 $Å^2$, and the framework can be simplified as a (3,4)-connected **tfj** network with the point symbol of $\{4.8^2\}_4\{4^2.8^4\}_2\{8^4.12^2\}$ topology. **2** shows a bi-pillared-layer type 3D framework based on 2D sheet of Zn(HL) and double Br-bdc pillars. Meanwhile, **1** exhibits a certain degree of CO_2 uptakes and selective CO_2/N_2 adsorption capacity. Furthermore, luminescent properties of **1a** well dispersed in different solvents have also been investigated systematically, which demonstrate distinct solvent-dependent luminescent spectra with emission intensities significantly quenched toward acetone and nitrobenzene. The result reveals that **1** could be applied as a fluorescence sensor for NB with high sensitivity, selectivity, and recyclability.

Acknowledgements

This work was financially supported by the NSFC of China (No. 21471027, 21171033, 21131001, 21222105), National Key Basic Research Program of China (No. 2013CB834802), Changbai mountain scholars of Jilin Province and FangWu distinguished young scholar of NENU.

Notes and references

Institute of Functional Material Chemistry, Key Laboratory of Polyoxometalate Science of Ministry of Education, Northeast Normal University, Changchun, 130024 Jilin, People's Republic of China. E-mail: qinc703@nenu.edu.cn; zmsu@nenu.edu.cn Fax: +86 431-85684009; Tel: +86 431-85099108.

† Electronic Supplementary Information (ESI) available: XRPD, IR, TG, photoluminescence spectra, N_2 sorption isotherm and additional figures. CCDC 1033030 (**1**) and CCDC 1033032 (**2**). For ESI and crystallographic data in CIF or other electronic format see DOI: 10.1039/b000000x/

1 (a) M. P. Suh, H. J. Park, T. K. Prasad and D. W. Lim, *Chem. Rev.*, 2012, **112**, 782; (b) K. Sumida, D. L. Rogow, J. A. Mason, T. M. McDonald, E. D. Bloch, Z. R. Herm, T. H. Bae and J. R. Long, *Chem. Rev.*, 2012, **112** , 724; (c) T. A. Makal, J. R. Li, W. Lua and H. C. Zhou, *Chem. Soc. Rev.*, 2012, **41**, 7761; (d) O. M. Yaghi, M. O'Keeffe, N. W. Ockwig, H. K. Chae, M. Eddaoudi and J. Kim, *Nature*, 2003, **423**, 705; (e) G. Férey, *Chem. Soc. Rev.*, 2008, **37**, 191; (f) S. Kitagawa and R. Matsuda, *Coord. Chem. Rev.*, 2007, **251**, 2490; (g) X. L. Wang, C. Qin, S. X. Wu, K. Z. Shao, Y. Q. Lan, S. Wang, D. X. Zhu, Z. M. Su and E. B. Wang, *Angew. Chem.*, 2009, **121**, 5395; *Angew. Chem., Int. Ed.*, 2009, **48**, 5291.

2 (a) Y. Cui, Y. Yue, G. Qian and B. L. Chen, *Chem. Rev.*, 2012, **112**, 1126; (b) M. Kim, J. F. Cahill, H. Fei, K. A. Prather and S. M. Cohen, *J. Am. Chem. Soc*., 2012, **134**, 18082; (c) D. Zhao, S. W. Tan, D. Q. Yuan, W. G. Lu, Y. H. Rezenom, H. L. Jiang, L. Q. Wang and H. C. Zhou, *Adv. Mater*., 20 11, **23**, 90; (d) B. Chen, S. Xiang and G. Qian, Acc. Chem. Res., 2010, 43, 1115; (e) M. Yoshizawa, J. K. Klosterman and M. Fu jita, *Angew. Chem., Int. Ed*., 2009, **48**, 3418; (f) D. M. D'Alessandro, B. Smit and J. R. Long, *Angew. Chem. Int. Ed*., 2010, **49**, 6058; (g) K. Sumida, M. R. Hill, S. Horike, A. Dailly and J. R. Long, *J. Am. Chem. Soc*., 2009, **131**, 15120; (h) J. R. Li, J. Sculley and H. C. Zhou, *Chem. Rev*., 2012, **112**, 869.

3 (a) C. Wang, D. Liu and W. Lin, *J. Am. Chem. Soc*., 2013, **135** , 13222; (a) S. Horike, M. Dincă, K. Tamaki and J. R. Long, *J. Am. Chem. Soc*., 2008, **130,** 5854; (b) M. Fujita, J. Y. Kwon, S. Washizu and K. Ogura, *J. Am. Chem. Soc.*, 1994, **116**, 1151; (c) L. J. Murray, M. Dinca and J. R. Long, *Chem. Soc. Rev*., 2009, **38**, 1294; (d) Z. R. Herm, J. A. Swisher, B. Smit, R. Krishna and J. R. Long, *J. Am. Chem. Soc*., 2011, **133**, 5664; (e) T. M. McDonald, W. R. Lee, J. A. Mason, B. M. Wiers, C. S. Hong and J. R. Long, *J. Am. Chem. Soc*., 2012, **134**, 7056; (f) R. Matsuda, R. Kitaura, S. Kitagawa, Y. Kubota, R. V. Belosludov, T. C. Kobayashi, H. Sakamoto, T. Chiba, M. Takata, Y. Kawazoe and Y. Mita, *Nature*, 2005, **436**, 238.

4 (a) X. L. Hu, C. Y. Sun, C. Qin, X. L. Wang, H. N. Wang, E. L. Zhou, W. E. Li and Z. M. Su, *Chem Commun*., 2013, **49**, 3564; (b) P. Horcajada, R. Gref, T. Baati, P. K. Allan, G. Maurin, P. Couvreur, G. Férey, R. E. Morris and C. Serre, *Chem. Rev*., 2012, **112**, 1232; (c) L. Q. Ma, J. M. Falkowski, C. Abney and W. B. Lin, *Nat. Chem*., 2010, **2**, 838; (d) B. L. Chen, Y. Yang, F. Zapata, G. N. Lin, G. D. Qian and E. B. Lobkovsky, *Adv. Mater*., 2007, **19**, 1693; (e) T. K. Maji, R. Matsuda and S. Kitagawa, *Nat. Mater.*, 2007, **6**, 142; (f) L. Pan, D. H. Olson, L. R. Ciemnolonski, R. Heddy and J. Li, *Angew. Chem.*, *Int. Ed*., 2006, **45**, 616.

5 (a) J. Z. Liao, D. C. Chen, F. Li, Y. Chen, N. F. Zhuang, M. J. Lin and C. C. Huang, *CrystEngComm*., 2013, **15**, 8180; (b) L. Tian, Z. Niu, Z. Y. Liu, S. Y. Zhou and P. Cheng, *CrystEngComm*., 2013, **15**, 10094 (c) K. Liu, Y. Peng, F. Yang, D. X. Ma , G. H. Li, Z. Shi and S. H. Feng, *CrystEngComm*., 2014, **16**, 4382; (d) X. L. Wang, N. Li, A. X. Tian, J. Ying, T. J. Li, X. L. Lin, J. Luan and Y. Yang, *Inorg. Chem*., 2014, **53**, 7118; (d) X. M. Zhang, T. Jiang, H. S. Wu and M. H. Zeng, *Inorg. Chem*., 2009, **48**, 4536; (e) Z. Sharifzadeh, S. Abedi and A. Morsali, *J. Mater. Chem. A*., 2014, **2**, 4803.

6 (a) H. Zhao, Z. R. Qu, H. Y. Ye and R. G. Xiong, *Chem. Soc. Rev*., 2008, **37**, 84; (b) J. R. Li, Y. Tao, Q. Yu and X. H. Bu, *Chem. Commun*., 2007, 1527; (c) Q. Ye, Y. M. Song, G. X. Wang, K. Chen, D. W. Fu, P. W. H. Chan, J. S. Zhu, S. D. Huang and R. G. Xiong, *J. Am. Chem. Soc*. , 2006, **128** , 6554; (d) M. Dincă, A. F. Yu and J. R. Long, *J. Am. Chem. Soc*., 2006, **128**, 8904; (e) Q. Ye, Y. H. Li, Y. M. Song, X. F. Huang, R. G. Xiong and Z. L. Xue, *Inorg. Chem*., 2005, **44**, 3618.

7 (a) M. Dincă, W. S. Han, Y. Liu, A. Dailly, C. M. Brown and J. R. Long, *Angew. Chem., Int. Ed*., 2007, **46**, 1419; (b) X. S. Wang, Y. Z. Tang, X. F. Huang, Z. R. Qu, C. M. Che, P. W. H. Chan and R. G. Xiong, *Inorg. Chem*., 2005, **44**, 5278; (c) Q. Ye, Y. Z. Tang, X. S. Wang and R. G. Xiong, *Dalton Trans*., 2005, 1570.

8 (a) J. P. Zhang, Y. B. Zhang, J. B. Lin, X. M. Chen, *Chem. Rev*., 2012, **112**, 1001; (b) J. P. Zhang, X. M. Chen, *J. Am. Chem. Soc*., 2008, **130**, 6010; (c) C. Yang, U. Kaipa, Q. Z. Mather, X. Wang, V. Nesterov, A. F. Venero and M. A. Omary, *J. Am. Chem. Soc*., 2011, **133**, 18094; (d) N. Nijem, P. Canepa, U. Kaipa, K. Tan, K. Roodenko, S. Takarli, J. Halbert, I. W. H. Oswald, R. K. Arvapally, C. Yang, T. Thonhauser, M. A. Omary and Y. J. Chabal, *J. Am. Chem. Soc*., 2013, **135**, 12615; (e) J. H. Wang, M. Li and D. Li, *Chem. Eur. J*., 2014, **20**, 12004; (f) N. M. Padial, E. Q. Procopio, C. Montoro, E. López, J. E. Oltra, V. Colombo, A. Maspero, N. Masciocchi, S. Galli, I.

Senkovska, S. Kaskel, E. Barea and J. A. R. Navarro, *Angew. Chem*., 2013, **125**, 8448 ; *Angew. Chem. Int. Ed*., 2013, **52** , 8290.
9 (a) W. Liu, T. Jiao, Y. Li, Q. Liu, M. Tan, H. Wang and L. Wang, *J. Am. Chem. Soc.*, 2004, **126**, 2280; (b) B. Gole, A. K. Bar and P. S. Mukherjee, *Chem. Commun.*, 2011, **47**, 12137; (c) N. Wei, Y. R. Zhang and Z. Bo. Han, *CrystEngComm.*, 2013, **15**, 8883.
10 P. Y. Wu, J. Wang, C. He, X. L. Zhang, Y. T. Wang, T. Liu and C. Y. Duan, *Adv. Funct. Mater*., 2012, **22**, 1698.
11 S. Pramanik, C. Zheng, X. Zhang, T. J. Emge and J. Li, J. *Am. Chem. Soc*., 2011, **133**, 4153.
12 G. M. Sheldrick, SHELXS 97, *Program for Crystal Structure Analysis*, University of Göttingen, Germany, 1997.
13 (a) G. M. Sheldrick, SHELXS 97, *Program for Crystal Structure Refinement*, University of Göttingen, Germany, 1997; (b) P. van der Sluis and A. L. Spek, *Acta Crystallogr. Sect. A* 1990, **46**, 194; (c) A. L. Spek, J. *Appl. Crystallogr.* 2003, **36**, 7.
14 A. L. Spek, PLATON, A multipurpose crystallographic tool Utrecht. University, The Netherlands, 2003.
15 (a) V. A. Blatov, A. P. Shevchenko, *TOPOS-Version 4.0 Professional (Beta Evaluation)*, Samara State University, Samara, Russia, 2006; (b) V. A. Blatov, A. P. Shevchenko, V. N. Serezhkin, *J. Appl. Crystallogr*. 2000, **33**, 1193;. (c) V. A. Blatov, *Struct. Chem*. 2012, **23**, 955.
16 (a) X. L .Hu, F. H. Liu, H. N. Wang, C. Qin, C. Y. Sun, Z. M. Su and F. C. Liu, *J. Mater. Chem. A*., 2014, **2**, 14827; (b) S. S. Kaye and J. R. Long, *J. Am. Chem. Soc*., 2005, **127** , 6506; (c) J. P. Zhang and X. M. Chen, *J. Am. Chem. Soc*., 2009, **131** , 5516.
17 (a) H. Kim, D. G. Samsonenko, S. Das, G. H. Kim, H. S. Lee, D. N. Dybtsev, E. A. Berdonosova and K. Kim, *Chem. Asian J*., 2009, **4**, 886; (b) M. Wriedt, J. P. Sculley, A. A. Yakovenko, Y. Ma, G. J. Halder, P. B. Balbuena and H. C. Zhou, *Angew. Chem. Int. Ed*., 2012, **51**, 9804; (c) D. Banerjee, Z. J. Zhang, A. M. Plonka, J. Li and J. B. Parise, *Cryst. Growth Des*., 2012, **12**, 2162.
18 Q. Zhang, A. Geng, H. Zhang, F. Hu, Z. H. Lu, D. Sun, X. Wei, C. Ma, *Chem. Eur. J*., 2014, **20**, 4885.
19 (a) Z. M. Hao, X. Z. Song, M. Zhu, X. Meng, S. N Zhao, S. Q Su, W. T. Yang, S. Y. Song and H. J. Zhang, *J. Mater. Chem. A.*, 2013, **1**, 11043; (b) Y. Q. Xiao, L. B. Wang, Y. J. Cui, B. L. Chen, F. Zapata and G. D. Qian, *J. Alloys Compd.*, 2009, **484**, 601.
20 (a) G. Y. Wang, C. Song, D.-M. Kong, W.-J. Ruan, Z. Chang, Y. Li, *J. Mater. Chem. A.*, 2014, **2**, 2213; (b) Y. C. He, H. M. Zhang, Y. Y. Liu, Q. Y. Zhai, Q. T. Shen, S. Y. Song, J. F. Ma, *Cryst. Growth Des*., 2014, **14**, 3174.